

**Supporting Information for**  
**Unprecedented Size-Sieving Ability in Polybenzimidazole Doped with Polyprotic Acids**  
**for Membrane H<sub>2</sub>/CO<sub>2</sub> Separation**

Lingxiang Zhu, Mark T. Swihart, and Haiqing Lin\*

Department of Chemical and Biological Engineering, University at Buffalo, The State  
University of New York, Buffalo, NY 14260, USA

\*Corresponding author. Tel: +1-716-645-1856, Email: [haiqingl@buffalo.edu](mailto:haiqingl@buffalo.edu) (H. Lin)

## Table of Contents

### 1. Experimental section

- 1.1 Materials
- 1.2 Preparation of PBI films
- 1.3 Preparation of acid doped PBI films
- 1.4 Characterization methods
- 1.5 Pure-gas permeation measurement
- 1.6 Mixed-gas permeation measurement

### 2. Supplementary results and discussion

- 2.1 Thermal gravimetric analysis (TGA) (**Figure S1**)
- 2.2 Fourier-transform infrared (FTIR) spectroscopic characterization (**Figure S2**)
- 2.3 Wide-angle X-ray diffraction (WAXD) characterization (**Figure S3**)
- 2.4 Manipulating acid doping level (**Table S1**)
- 2.5 Pure-gas transport properties (**Table S2**)
- 2.6 Gas sorption analysis (**Table S3**)
- 2.7 Determining fractional free volume (*FFV*) (**Table S4**)
- 2.8 Comparison of pure-gas and mixed-gas H<sub>2</sub>/CO<sub>2</sub> separation properties (**Table S5**)

### 3. References

## 1. Experimental Section

### 1.1 Materials

Celazole<sup>®</sup> PBI solution was provided by PBI Performance Products Inc. (Charlotte, NC, US). The solution contains about 9.5 wt.% PBI (with a molecular weight of 35,000 Da) in *N,N*-dimethylacetamide (DMAc). Phosphoric acid ( $\geq 98\%$ ), sulfuric acid (98%) and methanol (HPLC grade) were purchased from Thermo Fisher Scientific (Waltham, MA, US). Gas cylinders of H<sub>2</sub>, CO<sub>2</sub>, N<sub>2</sub> and CH<sub>4</sub> with ultrahigh purity were obtained from Airgas Inc., Buffalo, NY, US.

### 1.2 Preparation of PBI films

PBI thin films were prepared by a knife casting method using the following procedure. First, 4 mL of PBI solution was filtered using a 1.0  $\mu\text{m}$  PTFE syringe filter (Thermo Fisher Scientific, US). Second, the pretreated solution was cast on a glass plate using a casting knife (BYK-Gardner Inc., Germany) with a gate clearance of 200  $\mu\text{m}$ . Third, the wet film was dried overnight in a conventional oven at 60 °C under flowing N<sub>2</sub>, followed by heating at 200 °C under vacuum for 24 h. Finally, the resulting film was peeled from the glass substrate. The obtained films were about 10  $\mu\text{m}$  thick, as measured by a Starrett 2900 digital micrometer (The L.S. Starrett Co., MA, US).

### 1.3 Preparation of acid doped PBI films

Doping solutions were prepared by dissolving the desired amount of H<sub>3</sub>PO<sub>4</sub> (or H<sub>2</sub>SO<sub>4</sub>) in methanol. PBI films of mass  $m_0$  ( $\sim 150$  mg) were then immersed in the doping solution at 22 °C in a beaker. The solution was stirred by a 2.5 cm magnetic bar rotating at speed of 60 rpm. Each film was removed from the doping solution after 20 h, dried in a vacuum oven at 160 °C for 4 h, and weighed to determine its mass,  $m_1$ . There was no change in film appearance during this doping process. To achieve different doping levels ( $x$ ), the acid concentration in the doping

solution was varied from 0.05 to 1.0 wt.% and the mass ratio of acid and PBI was varied from 0.16 to 1.28, as summarized in **Table S1**. The doping level for each sample was determined using **Equation S1**:

$$x = \frac{(m_1 - m_0) / M_{Acid}}{m_0 / M_{PBI}} \quad (\text{S1})$$

where  $M_{PBI}$  (308 g mol<sup>-1</sup>) is the molecular weight of a PBI repeating unit, and  $M_{Acid}$  (98 g mol<sup>-1</sup>) is the molar mass of H<sub>3</sub>PO<sub>4</sub> or H<sub>2</sub>SO<sub>4</sub>.

#### *1.4 Physical characterization of PBIs doped with acids*

Attenuated-total-reflection Fourier-transform infrared (FTIR) spectra were recorded using an FTIR spectrometer (Vertex 70, Bruker, MA, US) over a wavenumber range of 600 to 4500 cm<sup>-1</sup> at a resolution of 4 cm<sup>-1</sup> for 100 scans. A Rigaku Ultima IV X-ray diffractometer was used to obtain Wide-angle X-ray diffraction (WAXD) patterns over a 2-theta range of 5 - 45° with a scanning rate of 2.0° min<sup>-1</sup>. The diffractometer has a Cu K $\alpha$  x-ray source with a wavelength of 1.54 Å. Thermal gravimetric analysis (TGA) was conducted using a SDT Q600 thermogravimetric analyzer (TA Instruments, DE, US) at temperatures from 30 to 900 °C with a heating rate of 10 °C min<sup>-1</sup> under flowing nitrogen.

The density of polymer films was determined at 23 °C using Archimedes' principle and an analytical balance (Model XS64, Mettler-Toledo, OH) equipped with a density kit. Iso-octane (>99 %, Thermo Fisher Scientific, Waltham, MA, US) was used as the auxiliary liquid.<sup>1</sup>

We used a Carl Zeiss Auriga<sup>®</sup> scanning electron microscope (SEM, Oberkochen, Germany) to examine the surface and cross-section of PBI films, and elemental analysis was performed using an energy-dispersive X-ray spectrometer (EDS, Oxford Instruments, Abingdon, UK) with the INCA analysis software. Before SEM-EDS characterization, the film cross-section was prepared by freeze-fracturing in liquid N<sub>2</sub>, and the sample was coated with gold using a sputter coating machine (Structure Probe Inc., PA, US).

Gas sorption isotherms of the polymer samples were determined using a high accuracy gravimetric sorption analyzer (IGA 001, Hiden Isochema, UK) at pressures up to 15 atm and 150 °C. The sample size for each measurement was around 100 mg, and the buoyancy effect on the mass reading was taken into account using Archimedes' principle.<sup>1, 2</sup> Before gas sorption measurement, the sample was dried overnight at 160 °C under vacuum to remove any guest molecules. The gas sorption values were determined from the equilibrated mass changes of the polymer samples with the corresponding compensation for buoyancy.

### 1.5 Pure-gas permeation measurement

The polymer film was masked using a brass disc and high-temperature epoxy adhesive to achieve an effective area for gas permeation of 3.9 cm<sup>2</sup>. A copper gasket was used to mount the sample in a permeation cell. This cell was assembled in a constant-volume and variable-pressure apparatus inside a temperature controlled oven at 150 °C. The leak rate in this apparatus was measured before starting the permeation experiments, and again afterward. Pure-gas permeability was determined by monitoring the steady-state rate of pressure increase in a fixed downstream volume ( $V_d$ ) using **Equation S2**:<sup>3, 4</sup>

$$P_A = \frac{V_d l}{p_{2,A} A R T} \left[ \frac{dp_{1,A}}{dt} - \left( \frac{dp_{1,A}}{dt} \right)_{leak} \right] \quad (\text{S2})$$

where  $l$  is the film thickness,  $A$  is the effective film area for gas permeation,  $R$  is the gas constant,  $T$  is the absolute temperature, and  $p_{2,A}$  and  $p_{1,A}$  are the upstream and downstream pressures, respectively.  $(dp_{1,A}/dt)$  is the steady-state rate of pressure increase in the downstream volume.  $(dp_{1,A}/dt)_{leak}$  is the system leak rate determined with both upstream and downstream volumes under vacuum, which was always less than 10% of  $dp_{1,A}/dt$  in this study. Each sample was measured at 3 different upstream pressures ranging from 8 to 15 atm, and the downstream region was always kept under vacuum (less than 0.02 atm), which was negligible relative to the feed pressure.

## 1.6 Mixed-gas permeation measurement

The mixed-gas permeability at 120 to 180 °C was determined using a constant-pressure and variable-volume apparatus.<sup>5</sup> SmartTrak<sup>®</sup> digital mass flow controllers (Sierra Instruments Inc., CA, US) were used to control the feed flow of 60 cm<sup>3</sup> (STP) min<sup>-1</sup> H<sub>2</sub> and 60 cm<sup>3</sup> (STP) min<sup>-1</sup> CO<sub>2</sub>, and a backpressure regulator was used to maintain the feed pressure of 14 atm. N<sub>2</sub> (2 - 4 cm<sup>3</sup> (STP) min<sup>-1</sup>) was employed as a sweep gas for the permeate stream at atmospheric pressure. The composition of the permeate and retentate were periodically analyzed using a 3000 Micro GC gas analyzer (Inficon Inc., Syracuse, NY, US). Gas composition results were recorded only after a steady state was reached. Mixed-gas permeability of gas component A can be calculated using **Equation S3**:<sup>4, 5</sup>

$$P_A = \frac{x_A S l}{x_{sweep} A (p_{2,A} - p_{1,A})} \quad (\text{S3})$$

where  $S$  is the flow rate of the sweep gas, and  $x_A$  and  $x_{sweep}$  are the mole fraction of gas component A and sweep gas (N<sub>2</sub> in this study) in the sweep-out stream, respectively.

The same setup was used to determine humidified-state mixed-gas permeability after attaching a humidifier to the feed gas line. The humidifier provided 0.042 atm water vapor to the gas stream with a total feed pressure of 14 atm at 150 °C. Consequently, the water content in the feed gas was 0.3 mol%. The composition of the permeate stream was analyzed periodically using the GC, and the humidified-state mixed-gas permeability was also calculated using **Equation S3**.

## 2. Supplementary results and discussion

### 2.1 Thermal gravimetric analysis (TGA)

**Figure S1** shows the TGA curves of PBI and a representative H<sub>3</sub>PO<sub>4</sub> doped PBI sample, PBI-(H<sub>3</sub>PO<sub>4</sub>)<sub>1.0</sub>. Both of the samples are thermally stable up to 200 °C, indicating their suitability for use at 150 °C for H<sub>2</sub>/CO<sub>2</sub> separation. Although the PBI backbones are not

expected to degrade below 500 °C,<sup>6</sup> this Celazole<sup>®</sup> PBI shows about 5.0 wt.% loss ( $\Delta m_1$ ) at 250 - 500 °C, presumably due to the degradation of impurities in this commercial PBI product. At 500 °C, PBI-(H<sub>3</sub>PO<sub>4</sub>)<sub>1.0</sub> loses 1.4 wt.% ( $\Delta m_2$ ) more mass than PBI, due to the decomposition of H<sub>3</sub>PO<sub>4</sub> to H<sub>4</sub>P<sub>2</sub>O<sub>7</sub> by removing H<sub>2</sub>O at around 250 °C.<sup>7</sup> The formation of H<sub>4</sub>P<sub>2</sub>O<sub>7</sub> can be described by



Both of the samples have massive weight loss above 500 °C, reflecting the degradation of their PBI backbones.<sup>6</sup>

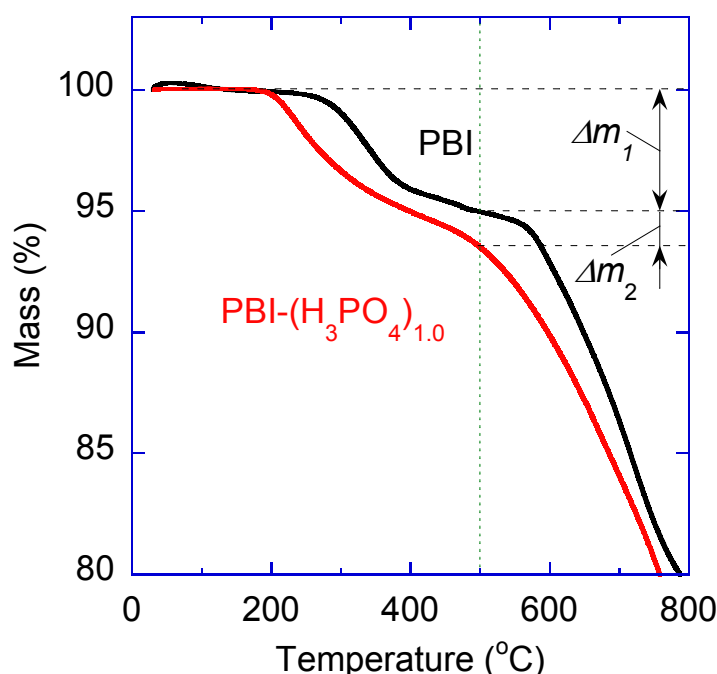


**Figure S1.** Thermal gravimetric analysis of PBI and a representative H<sub>3</sub>PO<sub>4</sub> doped PBI sample, PBI-(H<sub>3</sub>PO<sub>4</sub>)<sub>1.0</sub>.

## 2.2 Fourier-transform infrared (FTIR) spectroscopic characterization

**Figure S2** compares FTIR spectra of PBI and acid (H<sub>3</sub>PO<sub>4</sub> or H<sub>2</sub>SO<sub>4</sub>) doped PBI samples. The proton transfer from H<sub>3</sub>PO<sub>4</sub> onto nitrogen in PBI leads to the formation of H<sub>2</sub>PO<sub>4</sub><sup>-</sup>, indicated by its characteristic peaks of PO<sub>2</sub> (1050 cm<sup>-1</sup>) and P(OH)<sub>2</sub> (945 cm<sup>-1</sup> and 870 cm<sup>-1</sup>).<sup>8</sup> The protonation reaction between PBI and H<sub>2</sub>SO<sub>4</sub> is also confirmed by the formation of HSO<sub>4</sub><sup>-</sup>, indicated by the peaks at 865 cm<sup>-1</sup> [ $\nu$ (S-O) HSO<sub>4</sub><sup>-</sup>] and 1047 cm<sup>-1</sup> [ $\nu$ (S=O) HSO<sub>4</sub><sup>-</sup>].<sup>9</sup>

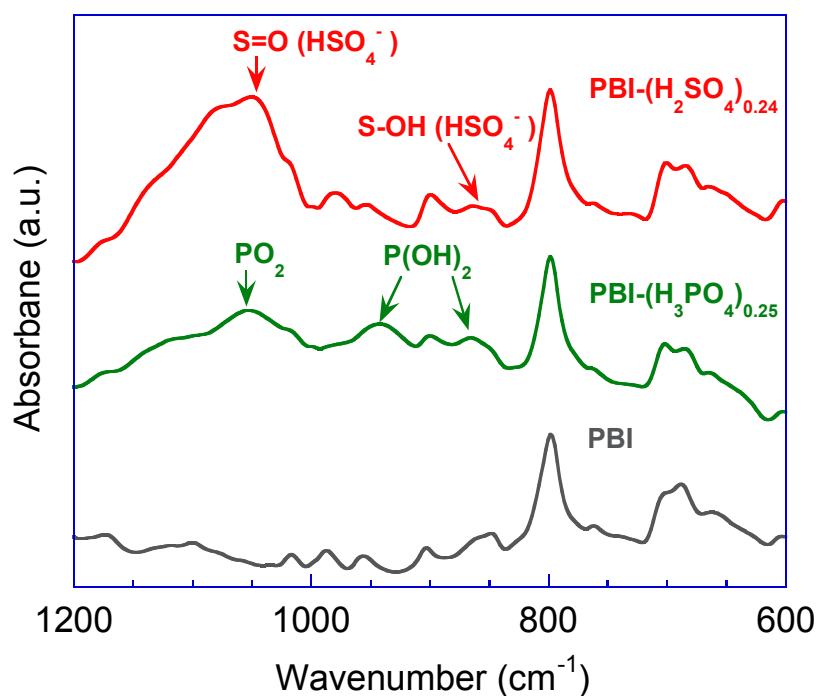


**Figure S2.** Comparison of the FTIR spectra of PBI, PBI-(H<sub>2</sub>SO<sub>4</sub>)<sub>0.24</sub> and PBI-(H<sub>3</sub>PO<sub>4</sub>)<sub>0.25</sub>.

### 2.3 Wide-angle X-ray diffraction (WAXD) characterization

The structural changes in polymer chain packing induced by acid doping were investigated using WAXD, as shown in **Figure S3**. PBI shows a diffraction peak at 22°, which corresponds to a *d*-spacing (or average inter-segmental distance between polymer chains) of 4.0 Å based on Bragg's law. Interestingly, both H<sub>3</sub>PO<sub>4</sub> and H<sub>2</sub>SO<sub>4</sub> doping shift the diffraction peak to 25°, which corresponds to a *d*-spacing of 3.6 Å. The result demonstrates that polyprotic acid (H<sub>3</sub>PO<sub>4</sub> or H<sub>2</sub>SO<sub>4</sub>) doping effectively reduces the interchain spacing via tight cross-linking.

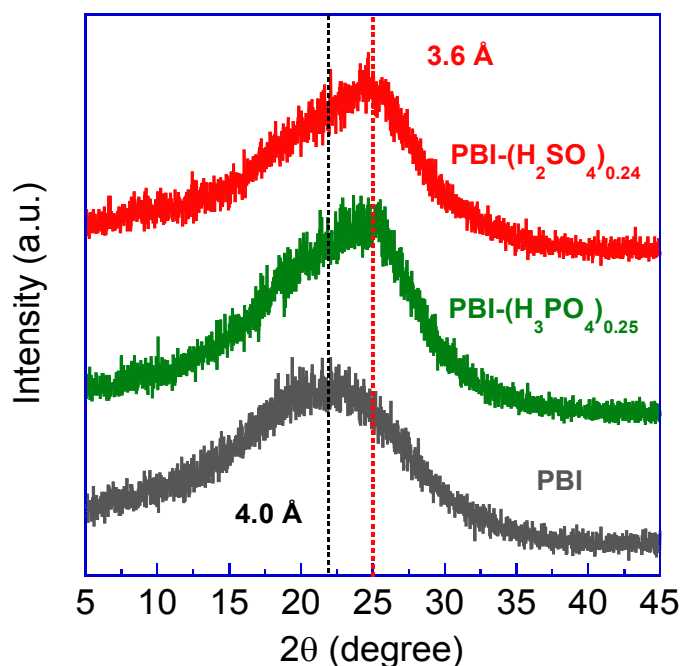


**Figure S3.** Comparison of WAXD patterns for PBI, PBI-(H<sub>2</sub>SO<sub>4</sub>)<sub>0.24</sub> and PBI-(H<sub>3</sub>PO<sub>4</sub>)<sub>0.25</sub>. The *d*-spacing is calculated based on Bragg's law.

#### 2.4 Manipulating acid doping level

The effect of initial acid concentration and acid/PBI molar ratio on the doping level was systematically investigated. The doping level for the resulting samples was determined using **Equation S1** and is summarized in **Table S1** below. Increasing initial acid concentration (or acid/PBI molar ratio) effectively increases the doping level. As a result, acid doped PBI samples with different *x* values (0.16-1.0) were obtained.

**Table S1.** Effect of initial acid concentration and acid/PBI molar ratio in the doping solutions on the doping level of the acid doped PBI samples.

Acid	Acid content in doping solution (wt.%)	Acid/PBI molar ratio	Doping level ( <i>x</i> )
H <sub>3</sub> PO <sub>4</sub>	0.05	0.5	0.16 ± 0.04
	0.05	1.0	0.25 ± 0.03
	0.10	2.0	0.45 ± 0.06
	0.20	2.0	0.65 ± 0.05
	0.40	2.0	0.82 ± 0.03
	1.00	4.0	1.0 ± 0.1
H <sub>2</sub> SO <sub>4</sub>	0.05	0.5	0.24 ± 0.05

## 2.5 Pure-gas transport properties

**Table S2** summarizes pure-gas H<sub>2</sub>/CO<sub>2</sub> separation properties of PBI and acid doped PBI samples at 150 °C. During the permeation measurement, the system leak rate was always less than 10% of the permeate flux, and the trans-film pressure varied from 8 to 15 atm. Gas permeability for each sample is independent of feed pressure, demonstrating these films are defect-free and resistant to CO<sub>2</sub> plasticization. Increasing the doping level decreases gas permeability while significantly increasing H<sub>2</sub>/CO<sub>2</sub> selectivity. For example, PBI-(H<sub>3</sub>PO<sub>4</sub>)<sub>1.0</sub> shows a remarkable selectivity of 140, which is much higher than the value of 16 obtained for pure PBI. At a similar doping level, PBI-(H<sub>2</sub>SO<sub>4</sub>)<sub>0.24</sub> and PBI-(H<sub>3</sub>PO<sub>4</sub>)<sub>0.25</sub> exhibit almost the same H<sub>2</sub> permeability and H<sub>2</sub>/CO<sub>2</sub> selectivity, presumably due to the similar effect of acids in enhancing chain-packing in PBI.

**Table S2** Pure-gas transport properties of PBI and acid doped PBI samples at 150 °C.

Acid	Doping level	H <sub>2</sub> Permeability (Barrer)			CO <sub>2</sub> Permeability (Barrer)			H <sub>2</sub> /CO <sub>2</sub> Selectivity
		8 atm	11 atm	15 atm	8 atm	11 atm	15 atm	
H <sub>3</sub> PO <sub>4</sub>	0	27	27	27	1.6	1.7	1.7	16
	0.16	12	12	12		0.34	0.34	35
	0.25	8.4	8.5	8.6	0.18	0.18	0.18	49
	0.45	6.0	6.1	6.1	0.10	0.10	0.10	61
	0.65	4.5	4.5	4.5		0.066	0.066	69
	0.82	2.5	2.6	2.5	0.031	0.031	0.030	84
	1.0	1.5	1.5	1.5		0.011	0.011	140
H <sub>2</sub> SO <sub>4</sub>	0.24	7.3	7.4	7.5	0.17	0.16	0.16	47

## 2.6 Gas sorption analysis

The isotherms in glassy polymers can be described using the dual mode sorption model, as expressed by **Equation S5**:<sup>10</sup>

$$C_A = k_D p_A + \frac{C'_H b p_A}{1 + b p_A} \quad (\text{S5})$$

where  $C_A$  is the sorption of the penetrant  $A$  in the polymer,  $k_D$  is the Henry's constant,  $C'_H$  is Langmuir sorption capacity, and  $b$  is the affinity parameter. **Table S3** summarizes the fitting

parameters for the CO<sub>2</sub> and CH<sub>4</sub> isotherms of PBI and PBI-(H<sub>3</sub>PO<sub>4</sub>)<sub>1.0</sub>. As shown in **Figure 3b**, the fitting lines agree well with the experimental data. Acid doping has minimal effect on gas sorption in PBI polymers as indicated by the similar fitting parameters for both PBI and PBI-(H<sub>3</sub>PO<sub>4</sub>)<sub>1.0</sub>.

**Table S3** Parameters of the dual mode sorption model for gas sorption in PBI and PBI-(H<sub>3</sub>PO<sub>4</sub>)<sub>1.0</sub> at 150 °C.

Gas	PBI			PBI-(H <sub>3</sub> PO <sub>4</sub> ) <sub>1.0</sub>		
	$k_D$ (cm <sup>3</sup> (STP) cm <sup>-3</sup> ·atm <sup>-1</sup> )	$b$ (atm <sup>-1</sup> )	$C'_H$ (cm <sup>3</sup> (STP) cm <sup>-3</sup> )	$k_D$ (cm <sup>3</sup> (STP) cm <sup>-3</sup> ·atm <sup>-1</sup> )	$b$ (atm <sup>-1</sup> )	$C'_H$ (cm <sup>3</sup> (STP) cm <sup>-3</sup> )
CO <sub>2</sub>	0.20	0.28	3.2	0.18	0.22	3.1
CH <sub>4</sub>	0.02	0.40	0.51	0.01	0.40	0.50

### 2.7 Determining fractional free volume (FFV)

The fractional free volume (FFV) can be determined using **Equation S6**:<sup>11</sup>

$$FFV = \frac{V - V_0}{V} = \frac{V - 1.3V_w}{V} \quad (\text{S6})$$

where  $V$  is the specific volume,  $V_0$  is the occupied volume, and  $V_w$  is the van der Waals volume, which can be estimated using the group contribution method.<sup>12</sup> For each acid doped PBI, we calculate its  $V_w$  value by considering the contributions from both acid (H<sub>3</sub>PO<sub>4</sub> or H<sub>2</sub>SO<sub>4</sub>) and PBI. The  $V$  values at 23 °C ( $V_{23^\circ\text{C}}$ ) can be derived from density measurement at 23 °C, while their values at 150 °C ( $V_{150^\circ\text{C}}$ ) are calculated based on thermal expansion theory using **Equation S7**:<sup>13</sup>

$$V_{150^\circ\text{C}} = V_{23^\circ\text{C}}(1 + \bar{\alpha}_V \Delta T) \quad (\text{S7})$$

where  $\Delta T$  (127 K) is the temperature difference, and  $\bar{\alpha}_V$  is the average volumetric thermal expansion coefficient in acid doped PBI samples. This  $\bar{\alpha}_V$  value can be estimated using

**Equation S8**:

$$\bar{\alpha}_V = \chi_1 \alpha_{V,1} + \chi_2 \alpha_{V,2} \quad (\text{S8})$$

where  $\chi_1$  and  $\chi_2$  are volume fractions of PBI and acid ( $\text{H}_3\text{PO}_4$  or  $\text{H}_2\text{SO}_4$ ) in acid doped PBI samples, respectively; and  $\alpha_{v,1}$  and  $\alpha_{v,2}$  are volumetric thermal expansion coefficients for PBI and acid, respectively. The  $\alpha_{v,1}$  value for PBI is  $6.9 \times 10^{-5} \text{ K}^{-1}$ , as reported by the manufacturer. The  $\alpha_{v,2}$  value is  $5.6 \times 10^{-4} \text{ K}^{-1}$  for  $\text{H}_2\text{SO}_4$ ,<sup>13</sup> and  $4.8 \times 10^{-4} \text{ K}^{-1}$  for  $\text{H}_3\text{PO}_4$  estimated from its density-temperature correlations at 25-170 °C.<sup>14</sup> The detailed values used to determine the *FFV* values at 23 °C and 150 °C are summarized in **Table S4**.

**Table S4** Calculation of the *FFV* values for polymers at different doping levels using the group contribution method.<sup>12</sup>

Acid	Doping level ( <i>x</i> )	$V_w$ (cm <sup>3</sup> mol <sup>-1</sup> )	$V_0$ (cm <sup>3</sup> mol <sup>-1</sup> )	23 °C			$\bar{\alpha}_V$ (10 <sup>-5</sup> K <sup>-1</sup> )	150 °C	
				Density (g cm <sup>-3</sup> )	$V_{23\text{ °C}}$ (cm <sup>3</sup> mol <sup>-1</sup> )	<i>FFV</i>		$V_{150\text{ °C}}$ (cm <sup>3</sup> mol <sup>-1</sup> )	<i>FFV</i>
H <sub>3</sub> PO <sub>4</sub>	0	154.6	201.0	1.288 ± 0.017	239.1	0.160 ± 0.017	6.9	241.2	0.167 ± 0.017
	0.16	160.9	209.1	1.353 ± 0.005	239.2	0.126 ± 0.009	8.3	241.7	0.135 ± 0.009
	0.25	164.4	213.7	1.370 ± 0.005	242.7	0.119 ± 0.007	9.0	245.5	0.129 ± 0.007
	0.45	172.3	223.9	1.405 ± 0.005	250.6	0.106 ± 0.011	10.6	254.0	0.118 ± 0.011
	0.65	180.1	234.2	1.436 ± 0.009	258.8	0.095 ± 0.011	12.0	262.8	0.109 ± 0.011
	0.82	186.8	242.8	1.457 ± 0.007	266.5	0.089 ± 0.007	13.1	271.0	0.104 ± 0.008
	1.0	194.7	253.1	1.498 ± 0.008	272.3	0.071 ± 0.012	14.4	277.3	0.087 ± 0.013
H <sub>2</sub> SO <sub>4</sub>	0.24	163.3	212.3	1.392 ± 0.005	238.2	0.109 ± 0.010	9.3	241.0	0.119 ± 0.012

## 2.8 Comparison of pure-gas and mixed-gas H<sub>2</sub>/CO<sub>2</sub> separation properties

**Table S5** compares the H<sub>2</sub>/CO<sub>2</sub> separation performance for pure-gas and binary mixed-gas (50% H<sub>2</sub>/50% CO<sub>2</sub>) measurements for PBI-(H<sub>3</sub>PO<sub>4</sub>)<sub>0.16</sub>, which provides a good combination of H<sub>2</sub> permeability and H<sub>2</sub>/CO<sub>2</sub> selectivity. Its mixed-gas separation properties are very close to the pure-gas separation performance at temperatures of 120, 150 and 180 °C, suggesting the absence of competitive sorption and plasticization in the acid-doped PBIs at high temperatures.

**Table S5** Comparison of pure-gas and mixed-gas H<sub>2</sub>/CO<sub>2</sub> separation properties in PBI-(H<sub>3</sub>PO<sub>4</sub>)<sub>0.16</sub> at different temperatures and a total feed pressure of 14 atm.

T (°C)	Pure-gas			Mixed-gas (50% CO <sub>2</sub> /50% H <sub>2</sub> )		
	H <sub>2</sub> (Barrer)	CO <sub>2</sub> (Barrer)	H <sub>2</sub> /CO <sub>2</sub> Selectivity	H <sub>2</sub> (Barrer)	CO <sub>2</sub> (Barrer)	H <sub>2</sub> /CO <sub>2</sub> Selectivity
35	0.65 ± 0.2	0.020 ± 0.002	32 ± 1			
120	7.4 ± 0.3	0.22 ± 0.02	34 ± 1	7.0 ± 0.3	0.21 ± 0.02	33 ± 2
135				9.0 ± 0.4	0.27 ± 0.02	33 ± 2
150	12 ± 1	0.34 ± 0.02	35 ± 1	12 ± 1	0.35 ± 0.02	34 ± 2
165				15 ± 1	0.48 ± 0.03	31 ± 2
180	18 ± 1	0.56 ± 0.03	33 ± 1	19 ± 1	0.60 ± 0.03	32 ± 2

## 3. References

1. L. Zhu, M. T. Swihart and H. Lin, *J. Mater. Chem. A*, 2017, **5**, 19914.
2. B. Lam, M. Wei, L. Zhu, S. Luo, R. Guo, A. Morisato, P. Alexandridis and H. Lin, *Polymer*, 2016, **89**, 1.
3. H. Lin and B. D. Freeman, *J. Membr. Sci.*, 2004, **239**, 105.
4. H. Lin and B. D. Freeman, in *Springer-Handbook of Materials Measurement Methods*, eds. H. Czichos, L. E. Smith and T. Saito, Springer, 2006, pp. 371.
5. T. C. Merkel, R. P. Gupta, B. S. Turk and B. D. Freeman, *J. Membr. Sci.*, 2001, **191**, 85.
6. X. Li, R. P. Singh, K. W. Dudeck, K. A. Berchtold and B. C. Benicewicz, *J. Membr. Sci.*, 2014, **461**, 59.
7. S. Samms, S. Wasmus and R. Savinell, *J. Electrochem. Soc.*, 1996, **143**, 1225.
8. X. Glipa, B. Bonnet, B. Mula, D. J. Jones and J. Roziere, *J. Mater. Chem.*, 1999, **9**, 3045.
9. R. Bouchet and E. Siebert, *Solid State Ionics*, 1999, **118**, 287.
10. S. Kanehashi and K. Nagai, *J. Membr. Sci.*, 2005, **253**, 117.
11. J. Y. Park and D. R. Paul, *J. Membr. Sci.*, 1997, **125**, 23.
12. A. Bondi, *J. Phys. Chem.*, 1964, **68**, 441.
13. R. H. Perry and D. W. Green, *Perry's Chemical Engineers' Handbook, Eighth Edition*, McGraw-Hill, New York, 2007.
14. D. I. MacDonald and J. R. Boyack, *J. Chem. Eng. Data*, 1969, **14**, 380.